ELEC4713 Final Report

Name: Renjie Dai

SID:490162237

The University of Sydney
Faculty of Engineering
School of Electrical and Information Engineering

Year S1, 2023

A thesis submitted in partial fulfilment of a Bachelor of Engineering Degree

Student Name	Renjie Dai
SID	490162237
Unit of Study Code and Name	ELEC4713 Thesis B
Supervisor	Cuo Zhang
Title	Battery energy storages system planning in an islanded microgrid

© Copyright 2020

The University of Sydney

SCHOOL OF ELECTRICAL AND INFORMATION ENGINEERING

PROJECT CLEARANCE FORM

Unit of Study Code and Name Elec4713 ThesisB

This is to certify that my student

Student Name Renjie Dai

SID 490162237

Has:

- **Returned all books and reference material;**
- **Returned all equipment and keys; and**
- **Tidied their work place.**

SUEIE Academic supervisor:

Signature:  **Date:** 02/11/23

Name: Cuo Zhang

ABSTRACT

The integration of large-scale renewable energy sources into the distribution network is a current and future trend. The clean, environmentally friendly, and renewable nature of renewable energy has led to an increase in the installed capacity of renewable energy generation. However, the output of renewable energy is closely related to weather and environmental factors and has a high degree of randomness and intermittency. In addition, the integration of large-scale renewable energy sources into the grid may lead to problems such as source-load imbalance in the distribution network, bidirectional flow of energy, and voltage and power fluctuations in the distribution network, which pose a great challenge to the control of the distribution network operation and the consumption of renewable energy sources. Battery energy storage technology has been maturely developed and widely used in actual production, which can effectively solve the above problems due to its advantages of fast response speed, peak shaving and valley filling, and flat wave suppression. However, the cost of battery energy storage is still relatively high, and it is necessary to consider the installation investment and operation and maintenance costs, etc., and the selection of the location and installation capacity of the battery energy storage system in the distribution network can directly affect the efficiency of battery energy storage. Therefore, how to plan for the location and capacity of battery storage in the distribution network to make the distribution network operate more economically and stably is a problem that must be solved nowadays. This paper is based on the study of battery energy storage system siting and capacity determination in the distribution network, and the main work is as follows: (1) Explain the design of battery energy storage system in the distribution network.

(1) The significance and importance of adding battery energy storage systems to distribution grids with a high proportion of renewable energy output is explained, and a brief overview of the current domestic and international research on battery energy storage systems and their siting and capacity is given.

(2) A deterministic model for the siting and capacity determination of battery energy storage systems in distribution networks is established. The optimization objective is to minimize the investment and operating costs discounted to one day, and the constraints mainly include the battery siting and capacity, battery operation constraints, and tidal current constraints, etc. The optimization objective is to minimize the investment and operating costs discounted to one day. Finally, the results are simulated in an IEEE-33 node distribution system with a high percentage of renewable energy and analyzed.

(3) A two-stage stochastic optimization method is introduced. The uncertainty of renewable energy output and load is simulated by generating relevant stochastic scenarios through Monte Carlo simulation, and the optimization objective is to minimize the ten-year total investment and operation cost by converting the deterministic model of battery storage siting and capacitation into a two-stage stochastic optimization model. Finally, a simulation is carried out in an IEEE-33 node distribution system with a high proportion of renewable energy, and the optimizations results are analyzed.

Table of Contents

1. Introduction

In recent years, with the rapid development of the global economy and industry, humanity's demand for energy has continued to rise, but traditional fossil fuels are facing the threat of gradual depletion. On the other hand, the extensive use of fossil fuels has led to excessive emissions of greenhouse gases and pollutants, exacerbating environmental pollution, disrupting ecological balance, and directly threatening human survival and development. Under the dual pressures of energy shortage and environmental degradation, nations worldwide have turned their focus to renewable energy sources to enhance energy utilization, improve energy structures, and realize sustainable energy development.

Renewable energy, compared to conventional sources, primarily includes wind, solar, marine, biomass, and geothermal energy. Among these, wind and solar power generation are the most rapidly developing and technically mature sectors of renewable energy. China possesses rich renewable energy resources. Actively developing and utilizing renewable energy generation has become a strategic choice for China to adjust its energy structure, protect the environment, respond to climate change, transform its economic growth mode, and realize sustainable development. At present, the approach to renewable energy development primarily follows two paradigms: "large-scale centralized development with medium and high voltage transmission" and "distributed development with low voltage local consumption". These correspond to two types of renewable energy generation: centralized large-scale generation and distributed generation. Centralized large-scale generation involves constructing large wind farms and photovoltaic power stations in areas abundant in renewable resources like wind and solar energy. This generated electricity is then transmitted directly into the main grid, which is currently the predominant form of renewable energy utilization. However, areas abundant in renewable energy, such as deserts and plateaus, are often far from urban load centers. Utilizing renewable energy in centralized large-scale generation necessitates long-distance electricity transmission, leading to energy loss and wastage. The randomly fluctuating active output can also affect the grid's reactive power balance, causing

significant voltage fluctuations along busbars. Moreover, the large-scale integration of renewable energy can impact the system's active power balance, intensifying stability challenges during grid disconnections.

In contrast to centralized generation, distributed generation (DG) refers to electricity produced using various scattered renewable sources (solar, biomass, wind, hydro, wave energy, etc.) and locally available fossil fuels (natural gas, coal, diesel, oil). The capacity is typically below 50 MW, and generation devices are installed close to the load. As distributed generation is near the load center, electricity can be consumed locally, reducing transmission losses, saving transmission infrastructure costs, and enhancing supply reliability and power quality. While DG primarily utilizes clean renewable sources, minimizing environmental impact, it also can employ various energy sources simultaneously for combined cooling, heating, and power, optimizing energy utilization efficiency. DG is flexible, meets the power needs of distributed loads, reduces the grid's installed capacity, and balances peak and off-peak demands.

Though DG has distinct advantages, it also poses challenges, such as high single-machine integration costs and complex control. Moreover, the uncontrollability and randomness of DG sources, as their penetration increases, can adversely impact power system stability. Currently, international standards mostly address DG as an uncontrollable source, imposing restrictions or isolations to mitigate its impact on the main grid According to IEEE 1547, DG sources must disconnect immediately during system faults, which significantly restricts the potential of DG.

To harmonize the relationship between the main grid and DG, attenuate DG's impact, and maximize its economic and environmental benefits, the concept of microgrids emerged. A microgrid integrates distributed sources, their loads, energy converters, protection, monitoring devices, and forms a small complete grid. It relies on controllable sources like energy storage

devices or diesel generators to maintain stability and integrate renewable sources like solar and wind. A microgrid has a common connection point (PCC) with the main grid. When the microgrid's output is insufficient, it can draw power from the main grid; when generating excess, it can feed it back. The primary distinction between DG integrated as microgrids versus direct grid integration is twofold: (1) Microgrids can control power flow direction at the connection point; (2) Microgrids can disconnect from the main grid, seamlessly transitioning between grid-connected and islanded modes, indicating the sophistication of microgrid operation technologies.

Figure 1 depicts a microgrid system. A microgrid is essentially a scaled-down version of the main power grid, tailored to provide electricity in a decentralized manner. One of the main features of a microgrid is its ability to operate in "island mode," which means it can function independently without relying on the primary grid.

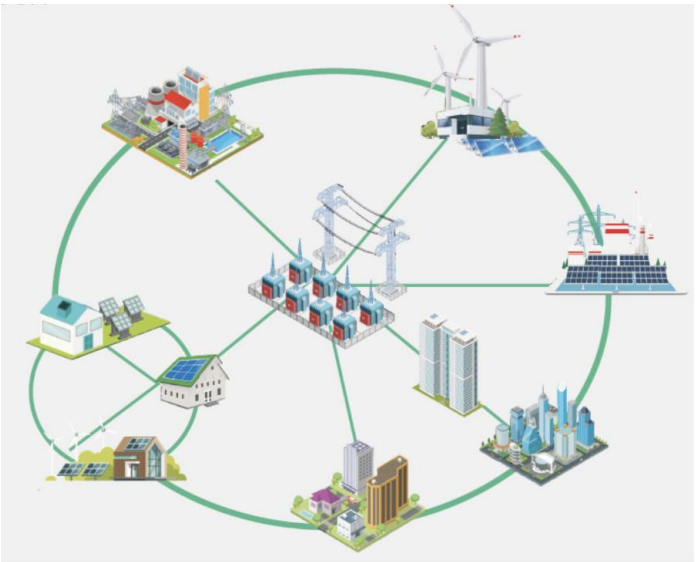

Figure 1 Integrated Microgrid Ecosystem

The need for microgrids, especially in mountainous areas, arises from their unique geography and infrastructure challenges. For regions like islands, mountainous terrains, or even the polar areas, where it's economically or technically challenging to connect with the main grid, establishing a microgrid can ensure a stable power supply. These areas might be remote or have conditions making them less accessible, and thus, a microgrid presents an effective

solution to their energy needs.

As a complementary form to the main grid, microgrids play a crucial role in catering to diverse end-user supply needs, enhancing energy utilization efficiency, and rapidly responding to load fluctuations. Recognized as the most effective organization of DG, microgrids have attracted widespread attention and are increasingly being adopted. Overall, the benefits of utilizing DG in the form of microgrids include:

(1) Enhanced system stability. Microgrids leverage internal energy storage and protective control to smoothen system outputs, maintain power balance, reduce, and overcome internal source fluctuations on the microgrid or main grid, and boost stability.

(2) Flexible power supply. Microgrids operate in grid-connected or off-grid modes, and the ability to switch between these enhances flexibility.

(3) Lowered grid investment costs. Microgrids are especially suitable for isolated regions where constructing a main grid is costly. Microgrids allow local electricity consumption, reduce transmission losses, save on infrastructure, and operation costs.

(4) Improved generation output. With diverse DG types in microgrids, their peak and off-peak generation times differ, complementing each other and resulting in a more balanced overall output.

(5) Increased energy utilization efficiency. Microgrids not only supply electricity but can also provide cooling, heating, or combined heat and power, enhancing energy efficiency.

(6) Enhanced supply reliability. With limited transmission scope, microgrids are more resilient to natural calamities. In grid-connected mode, if the main grid fails, microgrids can transition to off-grid mode, continue supplying power, and reconnect once the grid issue is resolved, significantly enhancing supply reliability.

In conclusion, microgrids inherit the advantages of DG and offer unique benefits. Integrating renewable energy resources into microgrids is a forward-thinking and viable way to utilize renewable energy. Microgrids exemplify an advanced stage in the evolution of energy systems

and are an essential component in the transition towards a sustainable and resilient energy future.

2Literature Review

2.1 Management Systems

The integration and management of microgrids present both a significant problem and an opportunity in the ever-changing field of renewable energy systems as we search for dependable and sustainable energy sources. Novel strategies to maximize efficiency and dependability are required due to the dynamic interactions of energy storage devices, renewable energy sources, and grid stability. This study explores important research endeavors that have made a substantial contribution to this topic, illuminating cutting-edge approaches and useful applications.

The study by Gomes, (2021) delves into the optimization of a renewable microgrid energy system, emphasizing the integration of energy storage.[6] The authors develop a comprehensive model that aims to enhance the operational efficiency and reliability of microgrids powered predominantly by renewable energy sources. The model addresses critical challenges such as the intermittent nature of renewable energy and proposes solutions for effective energy management and storage utilization. This research is pivotal for understanding the dynamics of renewable integration in microgrids and offers practical insights for real-world applications.

In their groundbreaking work, Nair, (2020) introduce a model predictive control-based energy management scheme tailored for hybrid storage systems in islanded microgrids.[14] The paper's core contribution lies in its novel approach to optimizing the operation of storage systems, thereby enhancing the stability and efficiency of microgrids. The authors provide a detailed analysis and simulation results to demonstrate the effectiveness of their proposed scheme, making a significant contribution to the field of microgrid energy management.

In this paper, Branco (2018) explores the critical role of battery energy storage systems in

integrating renewable energy sources into small, isolated power systems. [1] The paper addresses the technical and financial aspects of using battery energy storage to control the erratic and intermittent nature of renewable energy sources. This study is especially helpful since it offers a thorough examination of operational tactics and system design, which together offer a road map for the successful integration of renewable energy in standalone systems.

UNDRE (2019) focuses on the integration of high levels of renewable energy into the grid system and the balancing of islanded microgrids with battery energy storage systems.[19] The authors propose innovative solutions to maintain grid stability and efficiency, making this study an important reference for researchers and practitioners studying renewable energy integration and microgrid management.

Ryan's (2020) research introduces a novel data-driven control approach for grid-supported battery energy storage systems in isolated microgrids.[17] The authors' approach to control strategy design is both practical and forward-looking, providing new perspectives on how data can be used to optimize microgrid operation. These studies collectively highlight the importance of efficient energy storage and management systems in ensuring the stability and reliability of microgrids, particularly those with high reliance on renewable sources.

2.2 Optimization Methods

The objective of energy management in microgrid systems is to minimize the operational cost of distributed power sources, system power loss, etc., under the constraints of satisfying system load demands and various physical conditions, providing power operating points for distributed energy devices. For this purpose, commonly used energy optimization methods in microgrids include optimal scheduling, artificial intelligence techniques, and Model Predictive Control (MPC).

Optimal scheduling in microgrids can be categorized as a type of Mixed-Integer Nonlinear Programming (MINLP). Ghasemi (2016) addresses supply-demand balance by optimizing the charging and discharging time and quantity of energy storage and electric vehicles. [5]As the optimization problem includes both linear continuous and linear integer variables, it is solved using Mixed-Integer Linear Programming (MILP) methods. However, traditional optimization approaches have limited capabilities in handling complex nonlinear constraints, posing challenges in solving energy management optimization problems in microgrid systems. Consequently, researchers have proposed the use of heuristic algorithms to solve these energy optimization issues, including Genetic Algorithms and Particle Swarm Optimization (Raghavan, 2020).[16] jiraque (2021) focuses on the configuration optimization of renewable energy sources and batteries in islanded microgrids, establishing an optimization model targeting system operational costs, load mismatch capacity, and pollution emission costs.[8] This is solved using the NSGA-II multi-objective genetic algorithm. Additionally, other heuristic algorithms such as Differential Evolution, Immune Algorithms, and Ant Colony Optimization (ACO) (Geleta, 2021) [7] are used. Li (2015) applies an algorithm that combines Particle Swarm Optimization with chaos theory, enhancing the randomness and exploratory nature of particles, thereby achieving the global optimization goal of microgrid systems.[13] However, for energy management in microgrid systems, the optimization solving process involves a large number of nonlinear constraints, optimization variables, and interactive information with the system (Khan,2016), leading to a vast search space and the potential issue of dimensionality curse.[11] This makes these algorithms struggle with rapid convergence in solving energy optimization problems, hindering real-time decision-making.

With the rapid development of artificial intelligence technology, methods like deep learning and reinforcement learning have shown substantial advantages in various application scenarios (Duan, 2019).[3] These techniques have been widely applied in the field of microgrid energy management (Du, 2019).[4] Addressing the uncertainty in load electricity use within microgrid energy management systems, Xu (2020) proposes a predictive model

based on artificial neural networks, using multi-agent reinforcement learning for optimized decision-making for different loads.[20] Considering the low predictive accuracy of existing mathematical models for loads and renewable energy sources in practical energy management of microgrids, scholars suggest using reinforcement learning strategies for optimization scheduling. Domínguez (2020) combines deep neural networks with reinforcement learning, allowing the generation of power exchange strategies for microgrid systems under new input conditions without requiring user information, by training on historical data.[2] Ye (2020) introduces a model-free deep reinforcement learning algorithm to address the energy distribution problem between microgrid systems.[21] This algorithm approximates the scheduling policy directly through neural networks, eliminating the need for discretizing the state and action spaces. It also avoids the difficulties of direct space search using heuristic algorithms. Ji (2021) employs a deep reinforcement learning algorithm for online computation of energy optimization strategies, significantly improving the efficiency of microgrid electrical energy use.[10] Jayanetti(2022) further designs a deep reinforcement learning framework to solve complex energy coordination scheduling problems, enabling real-time energy management decisions and addressing the limitations of traditional iterative intelligent algorithms in real-time energy management optimization decisions[9].

MPC theory and its application represent a significant research topic in the development of control theory. Energy optimization methods in microgrids based on MPC have gained widespread attention in academia in recent years. Due to the uncertainties in renewable energy generation and plug-and-play load electricity use, and the need to solve optimal problems at every discrete time step with the optimal decision values applicable in the next time step, the MPC strategy is particularly suitable for energy management in microgrids. Keane (2012) introduces a rolling optimization control strategy to schedule available distributed generation energy, aiming to minimize the system's generation and environmental costs.[12] In Parisio,(2014), a new hybrid integer-linear method is embedded within the MPC framework, optimizing the economic cost of microgrid operation while meeting time-varying

demands and operational constraints.[15] For the optimization and coordination of energy supply and demand in multi-microgrid systems, Sharma (2016) propose an energy management framework based on MPC, not only reducing the operational costs of each subsystem but also ensuring the global system's supply-demand balance.[18]

In summary, the evolving field of energy management in microgrid systems is characterized by a diversity of approaches aimed at minimizing operational costs, power losses, and ensuring reliable load demand satisfaction under various constraints. These approaches primarily encompass optimal scheduling, artificial intelligence techniques, and MPC. These varied methodologies reflect the multifaceted nature of energy management in microgrid systems, highlighting the continuous evolution of strategies to address the intricate challenges posed by renewable energy integration and the ever-changing demand-supply dynamics in microgrids.

2.3 Operation Modes of the Microgrid

The operation modes of Microgrid are bifurcated into two: grid-connected and off-grid. For the grid-connected mode, the predominant control method is the PQ control, which maintains control over the active power by exchanging a constant tie-line power. Since the primary grid provides frequency support, tasks related to voltage regulation and frequency adjustment are typically accomplished by the main grid. Due to reactive power transmission occurring between the main grid and Microgrid and among the distributed power sources, it is imperative for the Microgrid to possess reactive voltage regulation capabilities when grid-connected, ensuring stable system operations.

During grid-connected operations, Microgrid can achieve energy complementation with the main grid. When there's a power mismatch between the distributed power generation and the load demand, the main grid supplies energy to maintain the power balance within the Microgrid, thus ensuring stable system operation. If the load demand is low, surplus energy

can be fed into the grid for economic gains.

In the event of a primary grid malfunction, Microgrid operates in islanding mode by disconnecting the PCC node. In this mode, each Microgrid can be perceived as an autonomous controllable unit with its decision-making and control capabilities, ensuring local load demand fulfillment and system stability, even when separated from the main grid. When operating in islanding mode, in the absence of main grid support, the focus for islanded Microgrid optimization should be real-time power regulation capabilities to smooth out power discrepancies between distributed micro sources and the load.

Islanded microgrids can be classified into scheduled islanding and unscheduled islanding. As per the IEEE1547-2003 standards, islanding operations compelled by grid malfunctions to limit the affected areas are termed unscheduled islanding. In such scenarios, Microgrid isolates from the rest of the grid, and the Microgrid autonomously resumes operations to ensure uninterrupted power supply to vital loads. Scheduled islanding refers to deliberate disconnection from the main grid by disconnecting the PCC node, aimed at preserving system stability and reliability. Unlike the grid-connected mode, Microgrid operating in islanding mode, devoid of main grid support, could experience significant frequency fluctuations. This necessitates effective frequency control strategies such as droop control, load shedding, or energy storage response settings, among others.

3 Methodology

Parameters and Variables Explanation:

Symbol	Description
P_{Gi}	Active power generated by generator i
P_{Gi}^{0}	Initial active power generated by generator i before any changes
ΔP_{Gi}	Change in active power generated by generator i
Δf	Change in frequency
m_{pi}	Coefficient relating change in frequency to change in active power for generator i
Q_{Gi}	Reactive power generated by generator i
Q_{Gi}^{0}	Initial reactive power generated by generator i before any changes
ΔQ_{Gi}	Change in reactive power generated by generator i
ΔUro	Initial change in voltage magnitude
S_i	Complex power at node i
$(P_{Li}$	Active power load at node i
Q_{Li}	Reactive power load at node i
I_i	Current at node i
	Voltage at node i

U_i	
I_{ij}	Current between nodes i and j
Z_{ij}	Impedance between nodes i and j
U_j	Voltage at node j
P_{LK}	Active power load constant
ΔU_r	Change in voltage magnitude
m_{qeq}	Equivalent coefficient relating change in voltage magnitude to change in reactive power
Q_{LK}	Reactive power load constant
Q_{G1}^0	Initial reactive power generated by generator 1
$\mathbf{I}_{\text{node}}$	Current vector at the nodes
I_{branch}	Current vector in the branches
U_{node}	Voltage vector at the nodes
U_{branch}	Voltage vector in the branches
Z_{branch}	Impedance vector of the branches
ΔU	Change in voltage

U^0	Initial voltage before any changes

3.1 Backward/Forward Sweep Algorithm for Microgrids

At the commencement of the Frequency Droop's Inner Loop algorithm, a pivotal step involves the preliminary assumption about the voltage nodes across the system. This presumption serves as the foundational basis on which subsequent calculations and evaluations are carried out. Specifically, these voltage nodes are perceived as static entities, believed to have been previously ascertained or inferred from prior system states. Essentially, this signifies that, before delving into the intricate layers of calculations, the algorithm is provided with a definitive voltage landscape that remains consistent throughout the procedure.

Objective Function:

The main objective is to minimize both the investment and operation costs of the system. The objective function can be represented as:

$$obj=inv + operation$$

where the investment might be associated with the setup costs (like purchasing of PV panels, battery storage systems, etc.) and the operation involves costs incurred during the daily functioning of the system (like maintenance, repairs, etc.).

Power Balance

At the heart of any efficient energy system lies the power balance equation. It ensures that at any given time, the energy produced and stored is commensurate with the energy consumed and lost. In the context of this PV and battery system, it means that the sum of power generated by the PVs, combined with power released from the battery during discharging, should equate to the sum of the load's power requirement and the power

used to charge the battery. The equation below

$$\sum_i \text{PMT} + \sum_i \text{PV} + \sum_i \text{Battery Discharging} = \sum_i \text{Load} + \sum_i \text{Battery Charging}$$

serves as a pivotal constraint, ensuring that the system neither faces a power deficit nor results in excessive energy wastage.

Energy Storage Dynamics:

The dynamics of energy storage is an intricate dance of charging and discharging, influenced by a multitude of factors. The equation provided tracks the evolution of energy within the battery across different time steps. At any given time t, the energy in the battery is the residual from the previous time step E_{t-1}, augmented by the energy from charging, and reduced by the energy used during discharging. However, it's not a straightforward addition or subtraction. The charging efficiency, represented by η and given as 0.99, plays a role. This means that not all the energy intended for storage is stored; a tiny fraction is lost, perhaps due to resistance or other inefficiencies. The equation below

$$E_t = E_{t-1} + \eta \cdot \text{Battery Charging} - \text{Battery Discharging}$$

thus, becomes pivotal in ensuring that the storage system operates optimally, providing energy when required and conserving it when not.

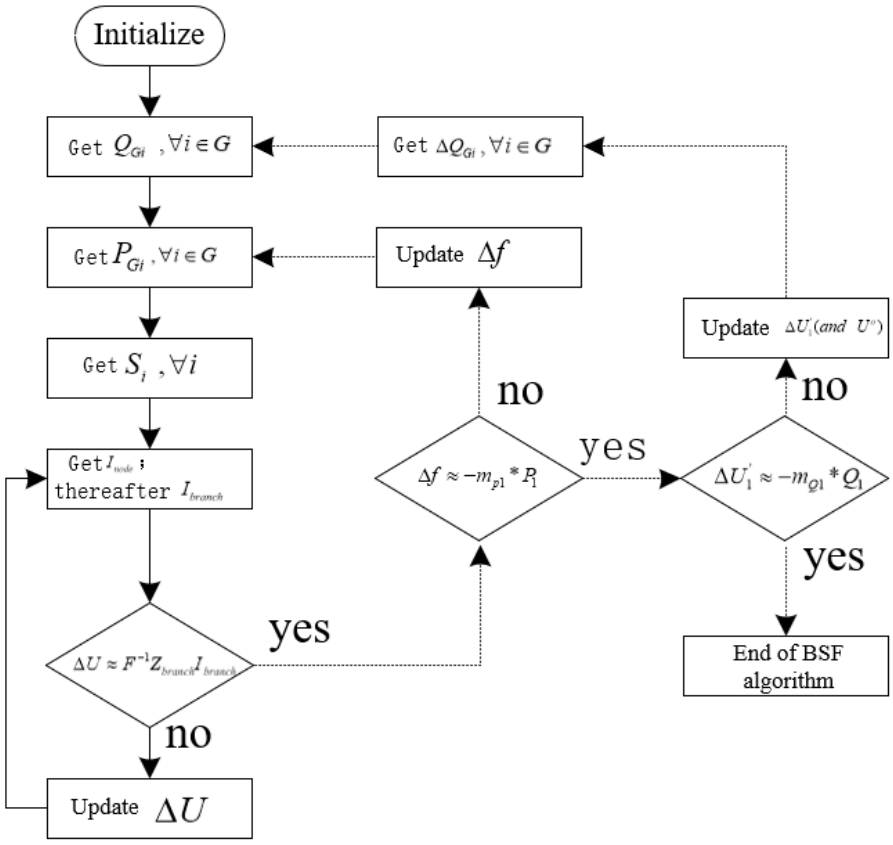

Figure2. Flow chart

Parallel to this, another integral parameter that is considered from the get-go is the deviation of the system's frequency from its nominal or baseline value, symbolically represented as Δf . The crux of this parameter lies in its ability to capture the nuances of frequency fluctuations, which is paramount for maintaining system stability and performance. The deviation is mathematically articulated as:

$$\Delta f = f - f^0 \quad (1)$$

Here, f stands for the current frequency, while f^0 denotes its nominal value. This frequency deviation serves as an essential guiding metric, driving subsequent computations, especially when assessing the required generation adjustments at each droop-regulated generator in the network.

To maintain the desired frequency level and uphold system stability, it's imperative to

calculate the required generation adjustments for droop-controlled generators. This is achieved by evaluating the deviation in power generation from its nominal or reference value. Mathematically, this deviation is described using the (2)

$$\Delta P_{G,i} = \frac{\Delta f}{m_{P,i}}, \text{ for } i = 2,\ldots,N \quad (2)$$

In this expression, $\Delta P_{G,i}$ represents the change in power generation for the i^{th} droop-controlled generator. This deviation is a function of the frequency deviation Δf and the droop characteristic coefficient $m_{P,i}$. The coefficient $m_{P,i}$ serves as a unique attribute for each generator, encapsulating the inherent response characteristic of the generator to frequency deviations. It's noteworthy that the index i commences from 2 and stretches up to N, suggesting that the equation is applicable for all droop-controlled generators from the second up to the Nth generator in the network. In essence, by using this formula, one can gauge the power adjustments required for each generator in order to counteract the observed frequency deviation and restore the system's balance.

In power systems, understanding the net power consumption at each node is crucial for efficient grid management and to ensure stability. To accomplish this, we need to consider both the active (real) and reactive components of the power, incorporating deviations in generation from their nominal values. The active and reactive power at a particular node can be defined using the following (3)

$$S_i = \left(P_{L,i} + \Delta P_{G,i}\right) + j\left(Q_{L,i} + \Delta Q_{G,i}\right), \text{ for } i = 2,\ldots,N \quad (3)$$

Here, S_i represents the complex power at the i^{th} node. The term $P_{L,i}$ denotes the real power load at the node, while $\Delta P_{G,i}$ signifies the deviation in real power generation. Similarly, $Q_{L,i}$ is the reactive power load, and $\Delta Q_{G,i}$ is the deviation in reactive power generation for the i^{th} node.

Breaking down the equation further, the real component $\left(P_{L,i}+\Delta P_{G,i}\right)$ gives us the net active power at the node, which is the algebraic sum of the real power load and the deviation in real power generation. Conversely, the imaginary component $j\left(Q_{L,i}+\Delta Q_{G,i}\right)$ calculates the net reactive power by combining the reactive power load with its respective deviation in generation. By determining the values for these components for each node, one can get a comprehensive picture of the power dynamics in the system. This detailed insight allows for better grid management and optimization, ensuring that the power supply meets demand efficiently while maintaining system stability.

Understanding the relationship between power and current is central to electrical engineering principles. This relationship is grounded in Ohm's and Kirchhoff's laws and can be described mathematically using complex power equations. In an AC system, where power comprises both active (real) and reactive components, the current, likewise, can have real and imaginary parts. As (4) provided.

$$I_i = \frac{S_i}{U_i}, \text{ for } i = 2,\ldots,N \quad (4)$$

which provides a way to derive the current, I_i, at a specific node, based on the complex power, S_i, and the voltage, U_i, at that node.

In (4), S_i is the complex power at node i. It combines both the real power (active power that does useful work) and the imaginary power (reactive power which is responsible for maintaining voltage levels and is not utilized in the actual work). The denominator, U_i, represents the voltage magnitude at the node. The resulting quotient provides the current, which reflects both the magnitude and the phase angle, at node i.

As we iterate through the nodes from $i = 2$ to N, this formula allows us to calculate the

current at each node, essential for subsequent network analysis steps. This process, thus, ensures that we have a holistic view of the current distribution throughout the system, facilitating deeper insights into system behavior and enabling effective optimization strategies.

Matrix computation is a powerful tool in the field of electrical engineering, especially when analyzing large and complex networks. In the context of electrical networks, a variety of matrices, such as the admittance matrix, impedance matrix, and node incidence matrix, play significant roles. One of the critical matrices is the node incidence matrix, denoted as Γ. This matrix essentially provides a relationship between nodes and branches in a network, allowing engineers to transition from nodal analyses to branch-focused investigations seamlessly. The given (5)

$$\mathbf{I}_{\text{branch}} = \Gamma^{-t}\mathbf{I}_{\text{node}} \quad (5)$$

indicates how we can calculate branch currents $\left(\mathbf{I}_{\text{branch}}\right)$ from node currents $\left(\mathbf{I}_{\text{node}}\right)$. Here, Γ^{-t} represents the inverse transpose of the node incidence matrix. The reason for this transformation (inverse transpose) is to convert nodal information to branch-specific details, as the relationship between nodes and branches in an electrical network is fundamentally a transpose relationship. By multiplying this transformed matrix with the node currents, we obtain the currents associated with each branch in the network.

In essence, this step ensures that we can transition our analysis from a nodal perspective to a branch-based one, which is vital for many analyses like fault detection, load flow, and network optimization. By determining the branch currents, we can get insights into how power flows through individual pathways within the system and make more informed decisions about system design and operation.

This algorithm delves into the relationship between frequency droop and the backward/forward sweep mechanisms. The backward sweep focuses on voltage nodes and

their correlation with the generation of droop-controlled generators. The forward sweep, meanwhile, refines bus voltages and leverages matrix computations for efficient derivation. Integrating this redesigned methodology into systems can streamline frequency droop computations, promoting efficient power distribution and stabilization.

In the realm of microgrid power flow analysis, our primary goal is to ensure steady power flow with uniform frequency distribution across the network. While our earlier methodology achieved this by considering a constant reference node voltage, U0, this isn't always a tenable assumption. Especially when considering voltage droops due to reactive power alterations, the system needs more adaptive mechanisms.

A voltage droop relationship, represented by $m_{Qi} = \left(\Delta U_i / \Delta Q_{Gi}\right)$, emphasizes that the voltage of the reference node isn't stagnant but is subjected to variations based on reactive power sharing. For a system with reference generator equipped with a voltage droop control, the voltage will inevitably deviate from the predefined value, particularly when the reactive power within the microgrid undergoes changes.

An initial approach was devised to update $\mathbf{U}^0$ for every conventional sweep - which we'll call the inner loop. This inner loop's main task is to compute bus voltages, updated as $\Delta\mathbf{U}$. However, simultaneous updates from voltage computations and reactive power alterations often conflicted, leading to oscillations or even divergence in certain situations.

During the forward sweep of our analysis, the droop characteristic of the reference generator becomes critical. As the grid encounters various reactive power shifts, the droop function acts as a sentinel, monitoring these variations and calculating the resultant voltage deviations, denoted as $\Delta U_i^{'}$. Each of these deviations, be it due to voltage or reactive power, are then methodically integrated into the inner loop. This systematic integration ensures that our power

flow analysis, despite any disturbances, gravitates towards achieving an equilibrium with every iteration. Thus, ensuring that the overall power distribution remains stable and consistent.

In a microgrid system, while the frequency parameter showcases a consistent behavior, voltage doesn't always exhibit the same uniformity. This disparity can lead to complications, especially when trying to maintain an equilibrium between voltage and the reactive power across different nodes of the grid. An intuitive approach to address this would be to meticulously iterate over each bus, aiming to strike the right balance between these two crucial parameters. However, this could be cumbersome and may not always guarantee optimal results.

An efficient alternative to this iterative approach leverages the equation:

$$\Delta \mathbf{U} = \mathbf{U}^0 + \Delta \mathbf{U}^{'} \quad (6)$$

By applying this equation, we bypass the need for exhaustive iterations. The beauty of this equation lies in its capability to determine the voltage values for the entire system based solely on the reference voltage. Such a matrix-centric operation not only simplifies the computational process but also enhances the accuracy of the voltage values deduced, fostering a more harmonious grid operation.

Post the operations of the inner loop, it becomes imperative to determine the voltage error, specifically at node 1. This is represented by:

$$\Delta U_1^{'} = -m_{Q1}\left[Q_{L1} + Q_{G1}^0 + \mathrm{Im}\left(\sum_{i \in \mathrm{A}_1} U_1 I_{1i}^* \right) \right] \quad (7)$$

Equation. (7) essentially captures the deviation in the voltage at the reference bus. Once this updated deviation is computed, it serves as a guidepost for the inner loop, alerting it about the new voltage level at the "slack" bus, represented by $U_1^0 - \Delta U_1^{'}$. Equipped with this adjusted voltage, the inner loop is better positioned to execute its subsequent calculations, ensuring a

streamlined power flow throughout the microgrid.

The described outer loop strategy efficiently integrates the voltage droop mechanism into our power flow analysis, ensuring a stable and adaptive power flow within the microgrid system. It not only counteracts the challenges posed by reactive power alterations but also paves the way for a more harmonized and resilient grid network.

3.2 GA Optimization for Battery Energy Storage Systems (BESS)

In the realm of modern electrical distribution systems, the integration of BESS has become increasingly crucial due to their potential to enhance grid stability and optimize energy utilization. This study is underpinned by a set of fundamental assumptions that guide its methodology and analysis. These assumptions are pivotal for the establishment of a coherent and applicable framework within which the optimization of BESS deployment is explored.

It is presupposed that prior to the commencement of this study, a Distribution System Operator (DSO) has meticulously evaluated the prospect of incorporating BESS into the distribution network. This analysis includes a detailed examination of financial limitations as well as an appraisal of the total advantages that BESS may provide to the power system. The DSO's evaluation is essential because it establishes the foundation for further choices on the kind and degree of BESS integration.

Every BESS unit is conceived and handled as a separate module with unique, predetermined features in this architecture. Aspects like storage capacity, charge-discharge rates, longevity, and efficiency may be included in these qualities. The maximum number of BESS modules that can be installed in the network has been set. When considering elements like space, cost, and system complexity, this limitation is crucial for assuring a feasible and controllable scope for BESS integration. The primary objective of this study is to optimize the allocation of BESS units across the network, both in terms of their quantity and strategic locations. This

study's main goal is to optimize the distribution of BESS units throughout the network in terms of both their quantity and key locations. This optimization targets power imbalances and voltage increase mitigation, especially in imbalanced battery distribution networks. An integral aspect of this goal is the enhancement of the hosting capacity (HC) of the distribution networks. The HC represents the network's ability to accommodate additional power sources, like renewables, without compromising on reliability or necessitating substantial infrastructure upgrades. By improving HC, the network's resilience, and adaptability to fluctuating power demands and generation profiles are significantly bolstered.

Battery Operating Constraints can be shown in (9)

$$\begin{aligned}
\beta_t^{ch} P^{B\min} \le P_t^{ch} \le \beta_t^{ch} P^{B\max}, \forall t \\
\beta_t^{\mathrm{dis}} P^{B\min} \le P_t^{\mathrm{dis}} \le \beta_t^{\mathrm{dis}} P^{B\max}, \forall t \\
\beta_t^{ch} + \beta_t^{\mathrm{dis}} \le 1, \forall t \\
E_t = \left(1-\delta^{sd}\right) E_{t-1} + \eta^{ch} P_t^{ch} \tau - P_t^{dis} \tau / \eta^{dis}, \forall t \\
SOC_t = E_t / E^{cap}, \forall t \\
SOC^{\min} \le SOC_t \le SOC^{\max}, \forall t
\end{aligned} \tag{9}$$

These constraints govern the operation of the battery system, including the limits on charging and discharging power, ensuring the battery is not charging and discharging simultaneously, updating the SOC, and maintaining SOC within its minimum and maximum limits.

The battery operating constraints are critical for the safe and efficient management of BESS. These constraints ensure that the batteries operate within their optimal capacity and longevity parameters. The first two constraints involve variables β_t^{ch} and β_t^{dis}, representing binary conditions for charging and discharging at any given time t. They dictate the permissible charging P_t^{ch} and discharging P_t^{dis} powers relative to their minimum $P^{B\min}$ and

maximum $P^{B\max}$ thresholds. These limits are essential to prevent overcharging or over-discharging, which can severely damage the batteries or reduce their lifespan. Additionally, the equation $\beta_t^{ch} + \beta_t^{\text{dis}} \le 1$ ensures that the battery cannot charge and discharge simultaneously, a critical aspect of battery management that prevents internal conflicts in power flow and potential damage to the battery system.

The SOC of a battery is a key factor in its operational management, indicating the current energy level relative to its total capacity. The equation $E_t = \left(1-\delta^{sd}\right)E_{t-1} + \eta^{ch}P_t^{ch}\tau - P_t^{dis}\tau / \eta^{\text{dis}}$ is central to updating the SOC. It takes into account the energy retained from the previous time period $\left(E_{t-1}\right)$, adjusted for any self-discharge $\left(\delta^{sd}\right)$, the energy added through charging $\left(\eta^{ch}P_t^{ch}\tau\right)$, and the energy subtracted due to discharging $\left(P_t^{\text{dis}}\tau / \eta^{\text{dis}}\right.$). Here, η^{ch} and η^{dis} are the charging and discharging efficiencies, respectively, and τ represents the time duration of each step. The subsequent equation $SOC_t = E_t / E^{cap}$ then computes the SOC as a ratio of the current energy level E_t to the battery's total capacity E^{cap}. The final set of constraints, $SOC^{\min} \le SOC_t \le SOC^{\max}$, ensure that the SOC remains within predefined limits, preventing situations where the battery is either too depleted or excessively charged. Maintaining the SOC within these bounds is crucial for preserving battery health, maximizing its lifespan, and ensuring it is always ready to supply or store energy as required by the grid's demands.

(1) GA Optimization Description

- In the context of the BESS allocation problem, a chromosome symbolizes a possible solution or configuration. It is essentially a blueprint that dictates how BESS units are distributed across a network.
- -For a distribution network comprising N nodes, a chromosome, denoted as C,

encapsulates this distribution. It is expressed as a vector $C = [x_1, x_2, \ldots, x_N]$.

- Each element x_i within this vector signifies the specific allocation of BESS at node i. This allocation can vary in its representation - it might denote the number of BESS units, the total capacity of these units, or even a binary indicator signifying the presence (1) or absence (0) of a BESS unit at the node.

Fitness Function

- The core of evaluating a solution in a genetic algorithm is the objective function, denoted as $f(C)$. This function assesses the quality or fitness of a given chromosome C.
- A conceivable form of this function could be $f(C) = \alpha \cdot$ PowerBalance $(C) + \beta \cdot$ VoltageDeviation (C), where PowerBalance (C) and VoltageDeviation (C) compute the power balance and voltage deviation for the given BESS configuration, respectively. The coefficients α and β act as weights, signifying the relative importance of each term in the overall evaluation.

Constraints Handling:

- Practical constraints are integrated into the genetic algorithm through penalty terms. These penalties discourage solutions that violate predefined constraints.
- For example, a constraint on the maximum BESS capacity $(\text{BESS}_{\max})$ at each node can be enforced by introducing a penalty term: Penalty $= \sum_{i=1}^{N} \max(0, x_i - \text{BESS}_{\max})$.
- The fitness function thus becomes an amalgamation of the objective and penalty terms: $f(C) = \alpha \cdot$ PowerBalance $(C) + \beta \cdot$ VoltageDeviation $(C) - \gamma \cdot$ Penalty, where γ is the penalty coefficient.
- Crossover: In single-point crossover, a pivot point p within the chromosome is randomly selected. Two parent chromosomes C^a and C^b exchange genetic material at this pivot to produce two new offspring chromosomes. This process combines traits

from both parents, potentially leading to better solutions.

- Mutation: Mutation introduces random alterations to a chromosome's genes, typically occurring with a low probability $P_{\text{mut.}}$. It's a crucial mechanism to maintain genetic diversity within the population. If a gene x_i undergoes mutation, it is modified as $x_i^{'} = x_i + \Delta$, where Δ represents a small, random variation. This process helps in exploring new regions in the solution space, which might be unattainable through crossover alone.

(2) GA optimization Algorithm Flow

- Initialization:

The algorithm starts with generating an initial population of chromosomes, each representing a unique BESS allocation configuration. This population, denoted as $\{C_1, C_2, \ldots, C_P\}$, is usually generated randomly, covering a broad range of potential solutions.

- Evaluation:

For each chromosome in the population, its fitness is calculated using the defined fitness function $f(C)$. This step assesses the viability of each solution in addressing the BESS allocation problem.

- Selection, Crossover, and Mutation:

The genetic algorithm then iteratively improves the population through the processes of selection (choosing the fittest chromosomes), crossover (creating new chromosomes by combining features of selected parents), and mutation (introducing random changes to maintain diversity).

- Termination:

The algorithm runs until a specific termination condition is met. This condition could be reaching a maximum number of generations, achieving a desired level of solution quality, or when the population's fitness ceases to improve significantly, indicating convergence.

4 Results and Analysis

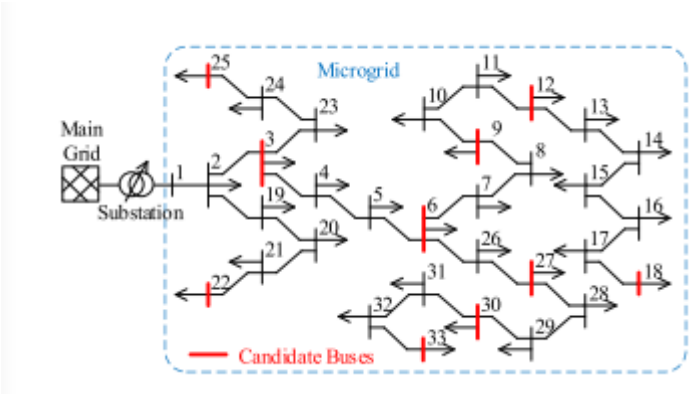

Figure3. Topology of test microgrid.

The test is based on the IEEE 33-bus, the IEEE 33 bus power distribution system is a widely used benchmark system in the field of power system research and analysis. It is an important test bed for testing and evaluating various power system analysis techniques, control strategies and optimization algorithms. This systematic introduction provides an overview of the IEEE 33-bus test system, including its main features, components, and applications in research and analysis.

Here is IEEE-33 bus data table in table 1:

Bus Numbe	ype of Bu	ted Bus	esistanc	Reactance	ower Loa	onductan	usceptan	ery Insta
1	1	2	0. 057526	0. 029761	0	0. 001	0. 0006	0
2	2	3	0. 307595	0. 156668	18	0. 0009	0. 0004	0
3	3	4	0. 228357	0. 1163	22	0. 0012	0. 0008	0
4	4	5	0. 237778	0. 121104	0	0. 0006	0. 0003	0
5	5	6	0. 510995	0. 441115	0	0. 0006	0. 0002	1
6	6	7	0. 116799	0. 386085	25	0. 002	0. 001	0
7	7	8	0. 44386	0. 146685	0	0. 002	0. 001	0
8	8	9	0. 642643	0. 461705	0	0. 0006	0. 0002	0
9	9	10	0. 648882	0. 461705	0	0. 0006	0. 0002	0
10	10	11	0. 122664	0. 040555	0	0. 00045	0. 0003	0
11	11	12	0. 233598	0. 077242	0	0. 0006	0. 00035	0
12	12	13	0. 915922	0. 720634	0	0. 0006	0. 00035	0
13	13	14	0. 337918	0. 444796	0	0. 0012	0. 0008	0
14	14	15	0. 36874	0. 328185	0	0. 0006	0. 0001	0
15	15	16	0. 465635	0. 340039	0	0. 0006	0. 0002	0
16	16	17	0. 80424	1. 073775	0	0. 0006	0. 0002	0
17	17	18	0. 456713	0. 358133	0	0. 0009	0. 0004	2
18	2	19	0. 102324	0. 097644	1	0. 0009	0. 0004	0
19	19	20	0. 938508	0. 845668	0	0. 0009	0. 0004	0
20	20	21	0. 255497	0. 298486	0	0. 0009	0. 0004	0
21	21	22	0. 442301	0. 584805	0	0. 0009	0. 0004	0
22	3	23	0. 281515	0. 192356	1	0. 0009	0. 0005	0
23	23	24	0. 560285	0. 442425	0	0. 0042	0. 002	3
24	24	25	0. 559037	0. 437434	0	0. 0042	0. 002	0
25	6	26	0. 126657	0. 064514	1	0. 0006	0. 00025	0
26	26	27	0. 17732	0. 090282	0	0. 0006	0. 00025	0
27	27	28	0. 660737	0. 582559	0	0. 0006	0. 0002	0
28	28	29	0. 501761	0. 437122	0	0. 0012	0. 0007	0
29	29	30	0. 316642	0. 161285	0	0. 002	0. 006	0
30	30	31	0. 607953	0. 60084	0	0. 0015	0. 0007	0
31	31	32	0. 193729	0. 225799	0	0. 0021	0. 001	4
32	32	33	0. 212759	0. 330805	0	0. 0006	0. 0004	0

4.1 BFS validation

Figure4. Real parts of the voltages at each node

Figure 3 includes the imaginary and real parts of the voltages at each node of the 33-node system after iterative calculation by the BFS algorithm, together with ΔU as defined in the thesis, including the real and imaginary parts of ΔU.

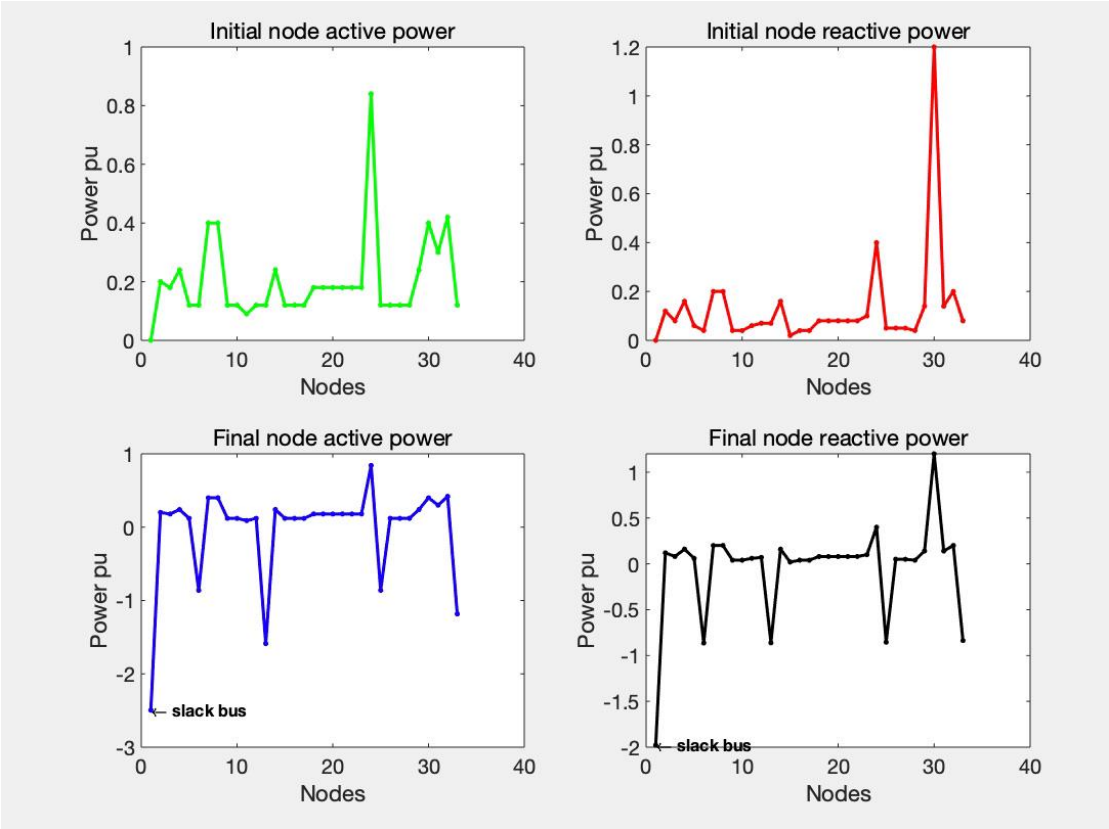

Figure5. Initial power and final power

Figure 4 includes the initial power at each node, both active and reactive, and the final active and reactive power at each node after the BFS algorithm.

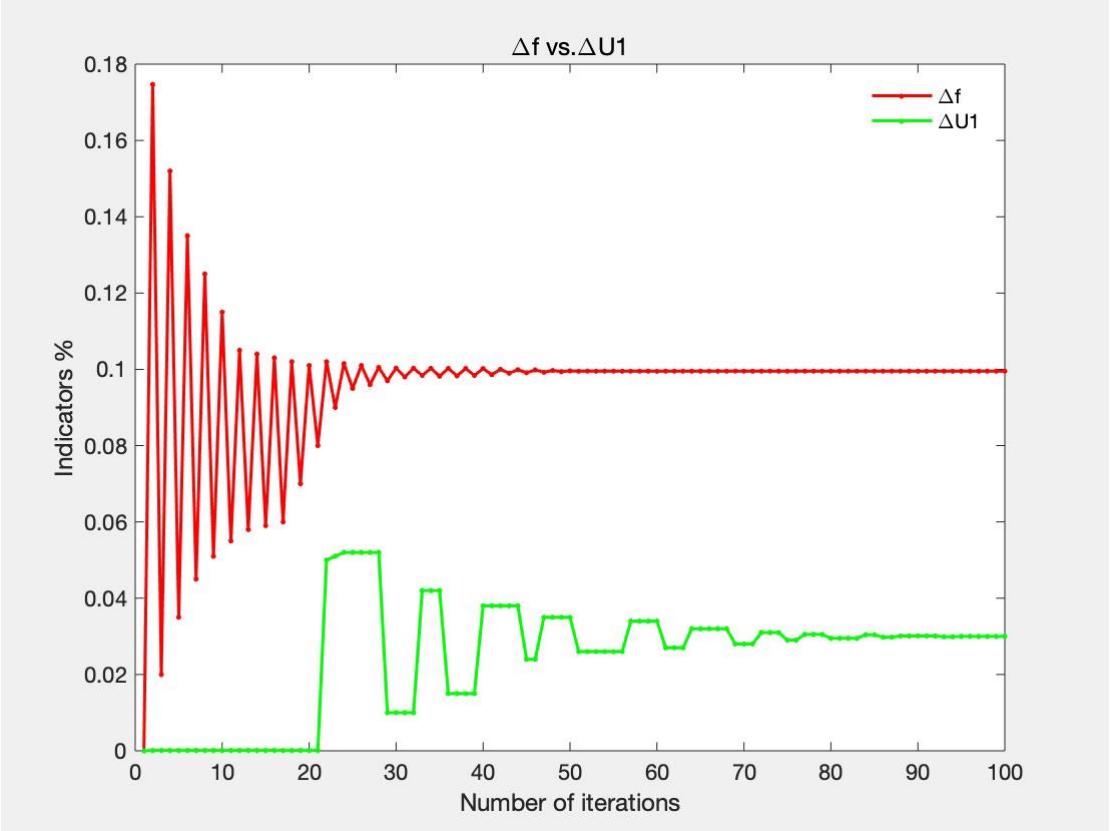

Figure6. Values of Δf and ΔU1

Figure 5 gives the process of changing the values of Δf and ΔU1 after iteration of the overall BFS algorithm, showing an oscillatory process, eventually converging to a fixed value, proving that the overall convergence of the algorithm is good.

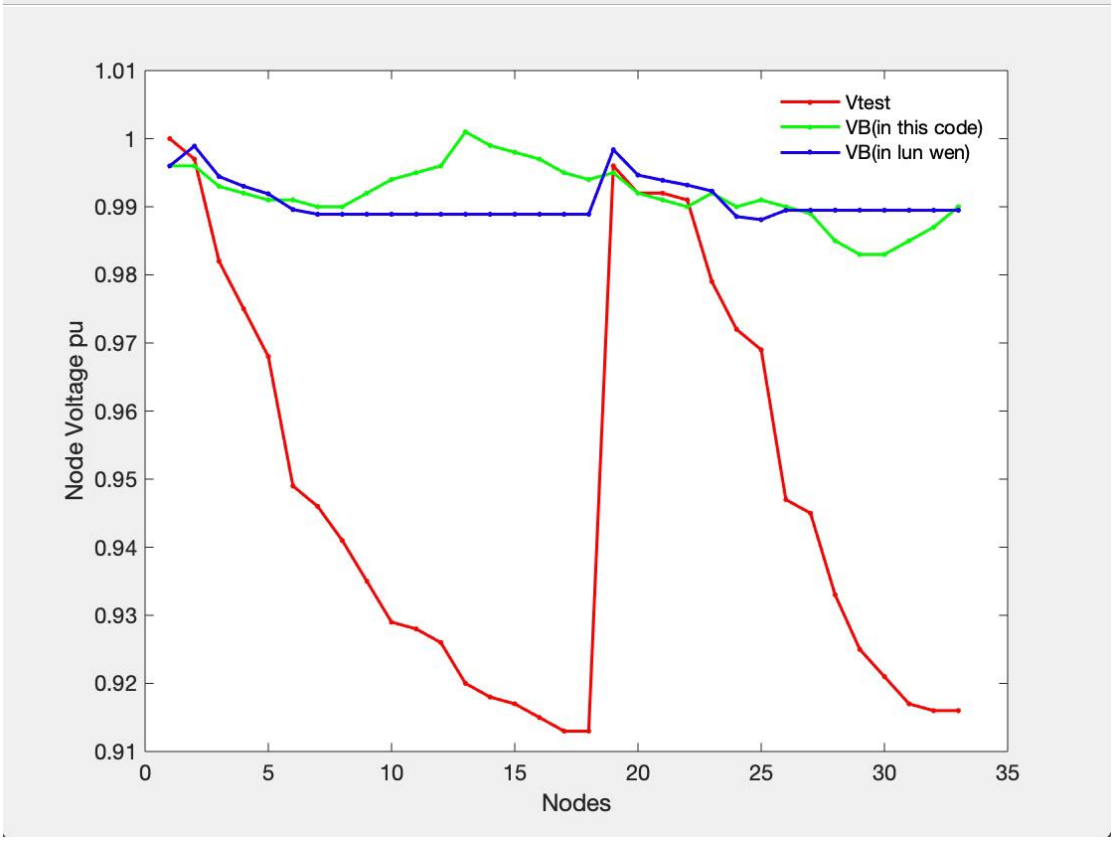

Figure7. Between the code and the thesis

Figure 7 shows the voltage comparison between the code and the thesis, the red line corresponds to fig4 of the thesis, which is the voltage of each node of the test system, the green one is the final presentation of our code, the blue one is the final voltage of each node of the thesis, the reason for the inequality is the impedance branch data, and the fact that the test system and the one given have different active and reactive power data for each branch, as well as some initial value effects

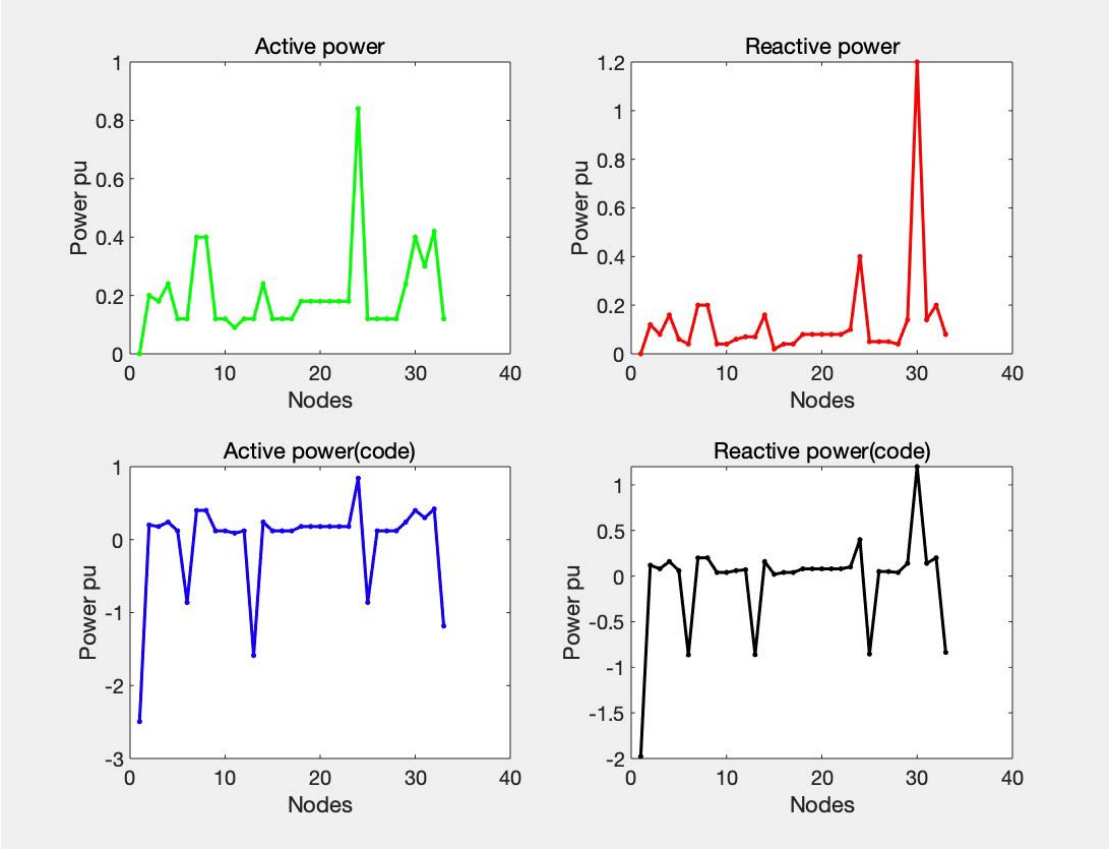

Figure8. Active and reactive power data

Figure 8 shows the active and reactive power data from the thesis compared with the active and reactive power data from our code, which, after continuous experimentation, can finally be reconciled to a consistent result.

4.2 Single and multiple candidate bus

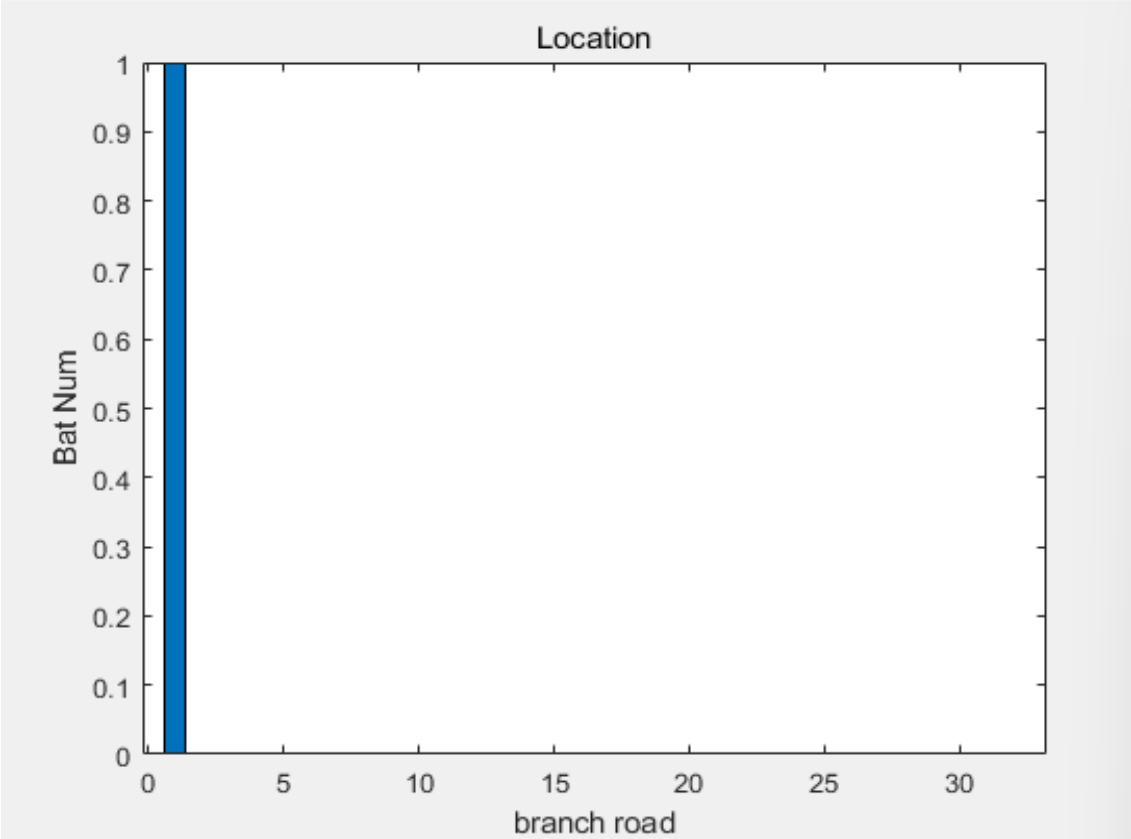

Figure 9 Distribution of Battery Installations in One Branch Roads

In the figure representing the installation of a single battery, we observe a pronounced peak at the very start, suggesting that most of the installations are happening close to the main junction or origin of the branch roads. As seen in this figure, the final choice was to install the battery energy storage system at nodes 1. The optimization results indicate that there are specific patterns or preferences for installing batteries at certain locations along feeder roads in a 33-bus system. These numbers may correspond to specific buses or locations identified as optimal battery installation points.

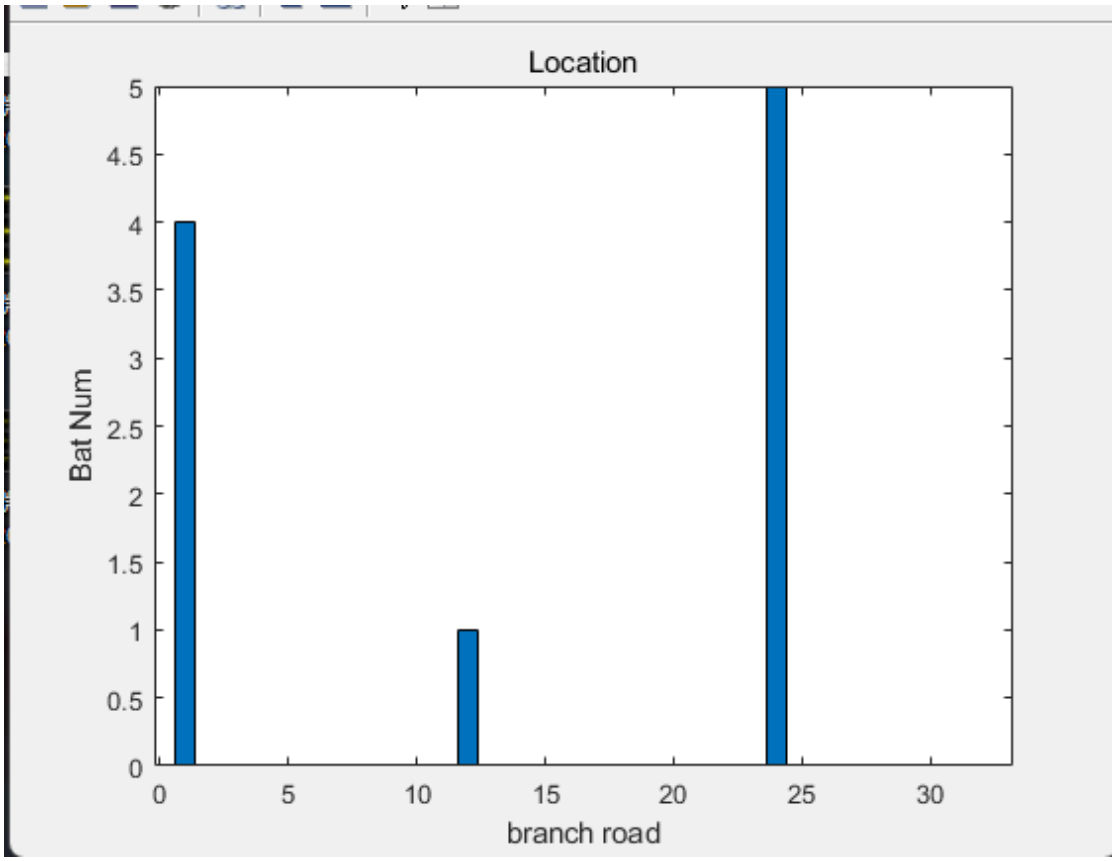

Figure 10 Distribution of Battery Installations in Different Branch Roads

As seen in this figure, the final choice was to install the battery energy storage system at nodes 1, 12 and 24, showcasing the distribution for ten batteries, a similar pattern is noticed. A significant peak is present at the beginning, indicative of a preference for installations near the main hub. However, there's an additional, smaller peak around the mid-point of the branch road, pointing towards a secondary preference for installations there. This might imply that while most batteries are being installed near the main road, there's also a considerable amount being placed at a central location along the branch roads. To surmise, the data underscores the strategic placement of batteries, predominantly at the start of branch roads. This could be due to factors such as ease of maintenance, accessibility, or proximity to power sources. The secondary peak in the ten-battery distribution could be a result of aiming to optimize battery placement for broader coverage or to cater to specific requirements in that area. Further investigation would be required to ascertain the exact reasons for this distribution, but it's clear that there's a method to the placement strategy being employed.

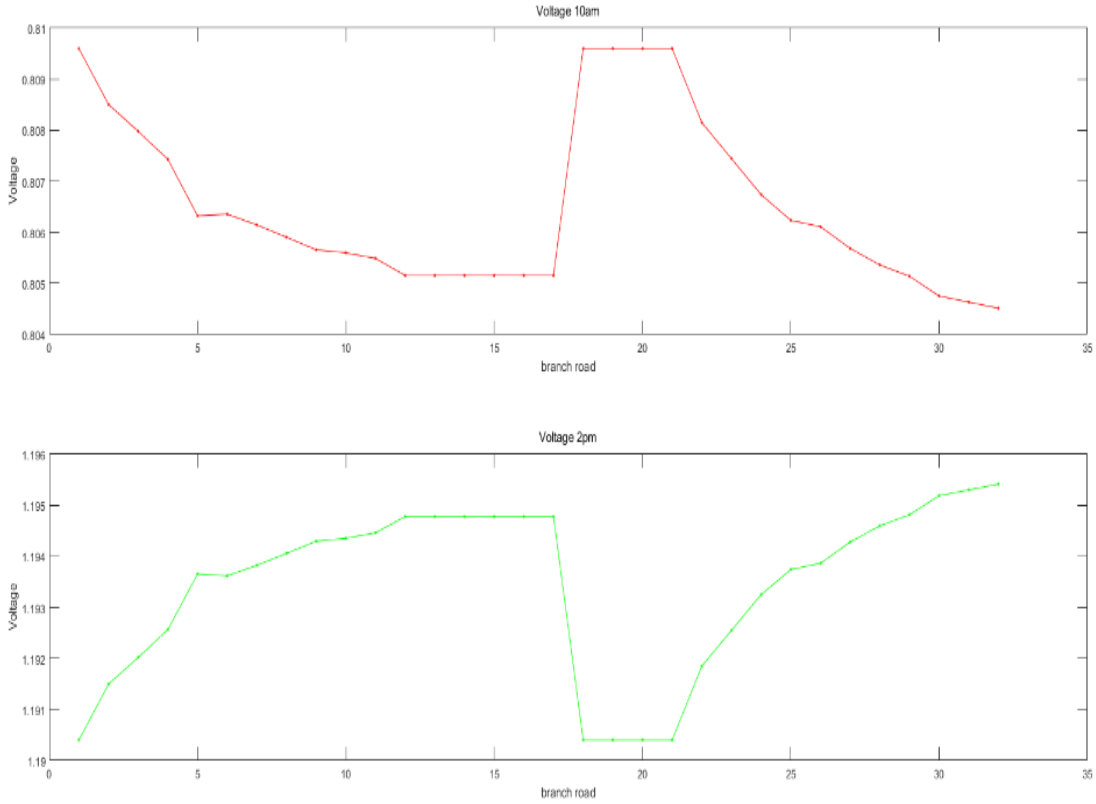

Figure 11. Voltage Fluctuations at 10am and 2pm

Figure11 showcases a significant drop in voltage as we move from the start of the branch road to around the 15th marker. After this point, there is a sharp spike that peaks near the 20th marker, only to fall sharply again as it approaches the 25th marker. The trend continues with a steady decline towards the end of the graph. This suggests that during the morning hours, there are regions on the branch road that experience higher voltage demands or potential system inefficiencies leading to these fluctuations. The voltage levels in the afternoon follows a different trend. Starting off, there's a moderate increase in voltage until the 15th marker. A sudden drop occurs around the 20th marker, followed by a steady rise as we approach the end of the branch road. This indicates that there may be less demand or better distribution of resources during the afternoon hours compared to the morning. When comparing the two times of the day, it's evident that the voltage stability varies, with the afternoon seemingly having a smoother curve despite its mid-graph drop. It's essential to consider these

fluctuations when planning power distribution and ensuring efficient energy usage throughout the branch road.

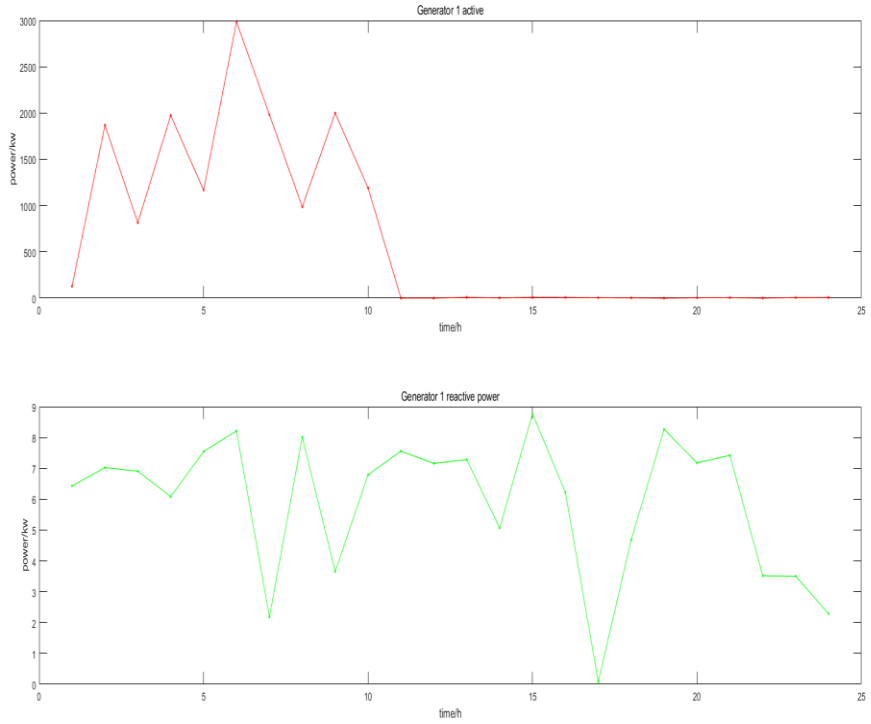

Figure12. Power Output Analysis of Five Generators

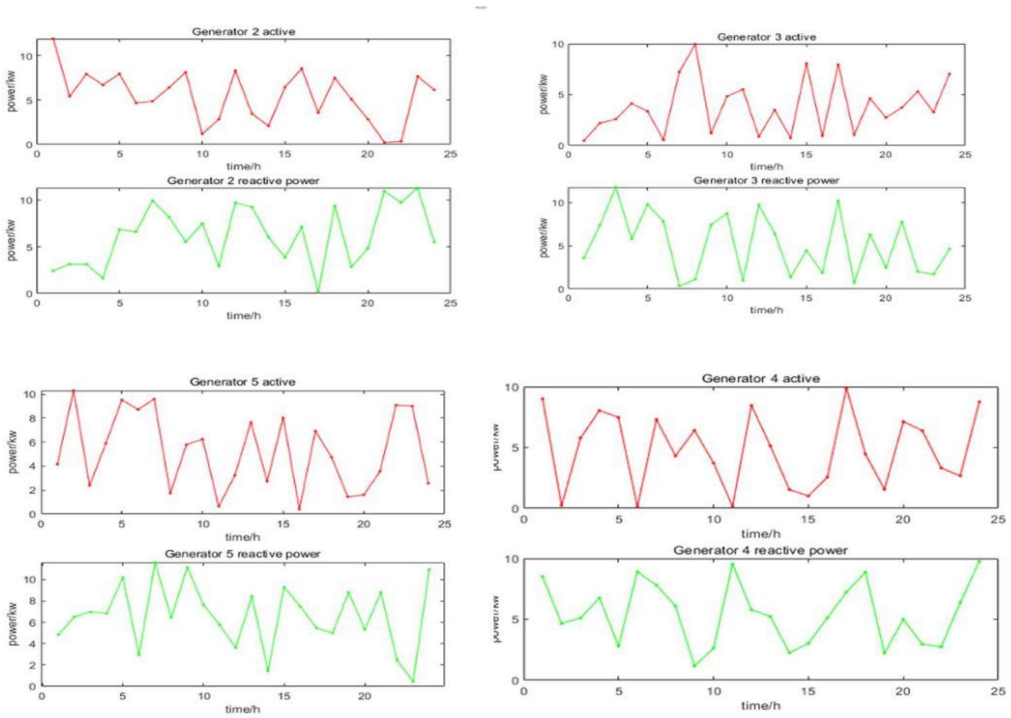

Figure 13. Power Output Analysis of Five Generators

Five different generators' outputs of active and reactive power over time are shown in Figures 12 and 13. Every generator has a different power output pattern, which offers important information about how efficiently they operate as well as possible areas for improvement. A cursory examination of the active power graphs reveals that the power output of each generator oscillates on a regular basis. Generator 2 and Generator 5, for instance, demonstrate a relatively consistent amplitude in their active power output, while Generators 3 and 4 exhibit greater variability. This suggests that some generators maintain a more stable output, which could be attributed to factors such as newer equipment or more efficient operational procedures. In terms of reactive power, all generators show a similar sinusoidal pattern, indicating potential synchronization or shared operational conditions. The reactive power output for Generator 2 and Generator 3 mirrors each other closely. A closer examination of the reactive power trends might reveal areas where adjustments can be made to improve power factor and overall system efficiency.

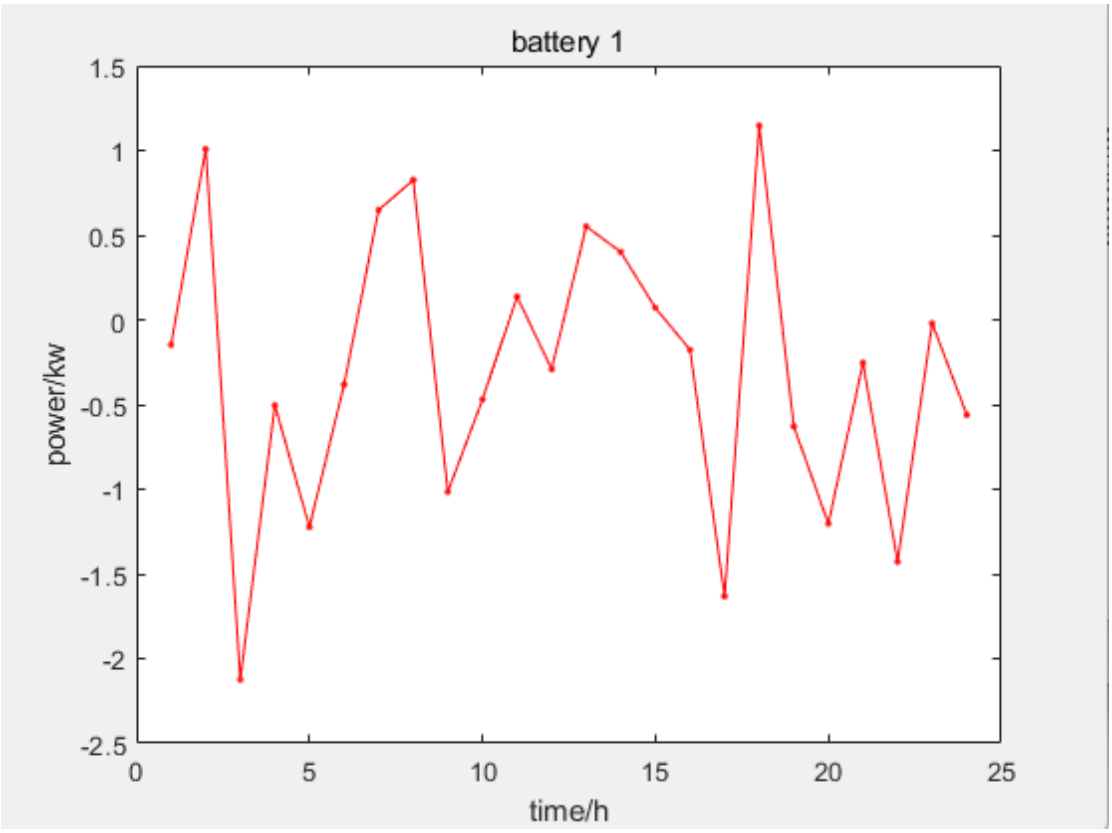

Figure 14. Battery1 Charging and Discharging

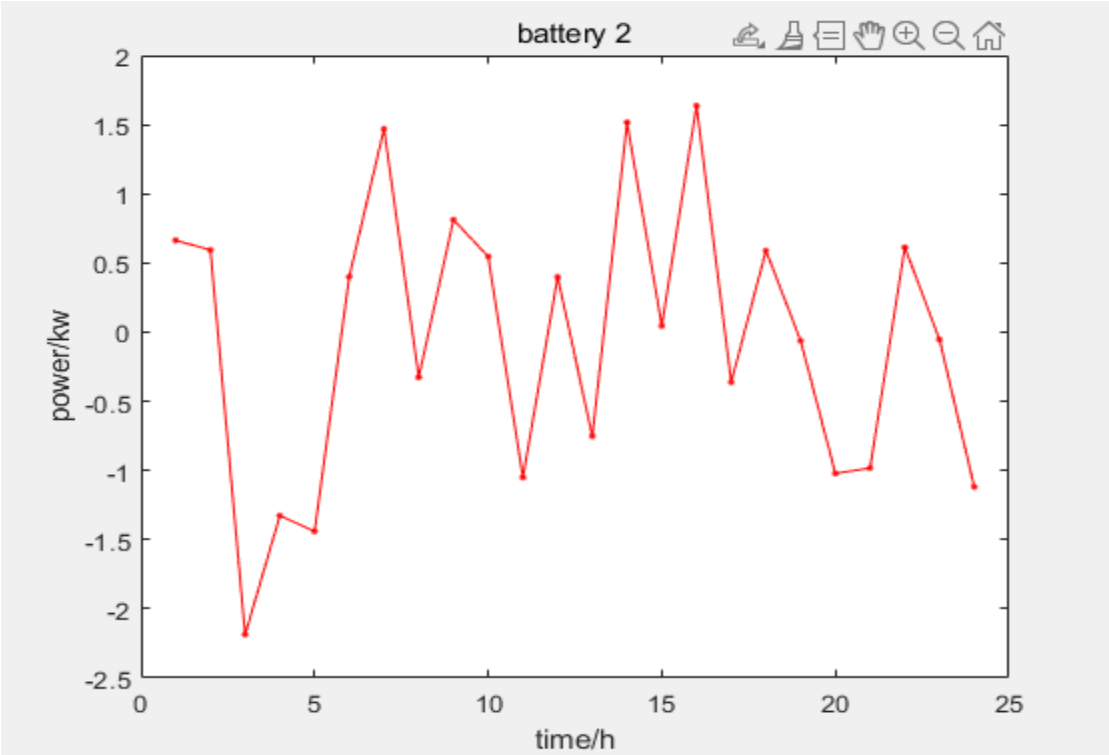

Figure 15. Battery2 Charging and Discharging

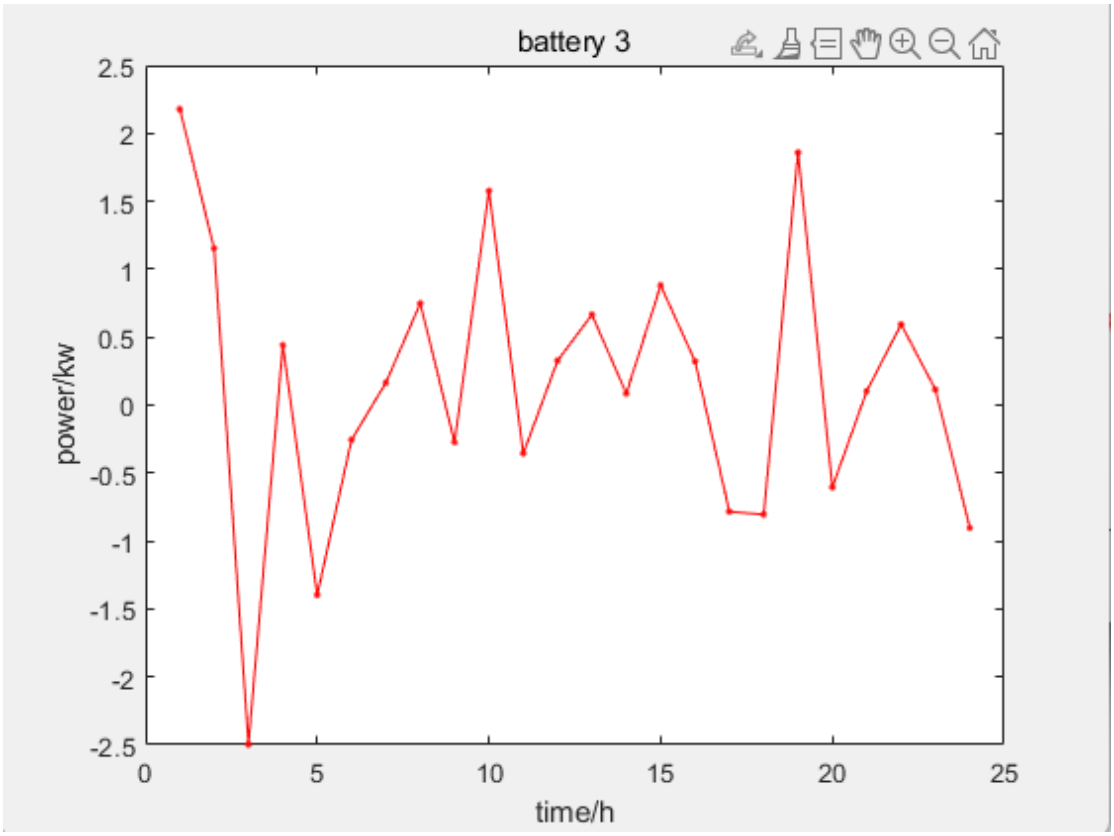

Figure 16. Battery3 Charging and Discharging

Figure 14 to 16 provides a detailed visualization of the charging and discharging patterns observed in three different batteries over a 24-hour period. All three batteries exhibit distinct power ranges and cycles, shedding light on their respective capacities and operational behaviors. Upon analyzing the curves, it is evident that each battery experiences both charging and discharging phases. Battery 1 operates within a range of approximately 1.5 kW, whereas Battery 2 and Battery 3 display more pronounced variances with peaks nearing 2 kW and 2.5 kW, respectively. The similar sinusoidal patterns across the three graphs suggest a coordinated charging and discharging strategy, possibly to balance the load or respond to external demand cycles. The consistent patterns of these batteries may indicate the implementation of a standardized charging algorithm or a response to a regular demand cycle. Evaluating the efficiency, capacity, and longevity of each battery in relation to these patterns could provide insights into optimal charging strategies and potential areas for improvement. Future analyses might also consider the effects of external factors such as temperature, usage patterns, and battery age on these observed behaviors.

These are some factors might affect the battery charging and discharging wave:
Generator effects on battery charging and discharging.
During the charging, if the generator output is lower than the power required to charge the battery, the battery may not charge or may charge at a slower rate. When the generator output is higher than expected, the battery may charge too quickly, which may lead to overheating or other safety issues.

And during the discharging, when generator power is insufficient to meet load requirements, the battery will be used to make up the shortfall, which may result in more frequent discharges. If the generator suddenly returns to normal output, battery discharge may be interrupted, and this discontinuous discharge pattern may affect battery performance and life.

PV effects on battery charging and discharging.

During the charging, when there is sufficient sunlight, the PV system may generate a large amount of power that exceeds the real-time load demand, and the excess power will be used to charge the BESS. If the light decreases and the PV generation drops, it may not be able to meet both the load and charging BESS demand, at which point the BESS may need to be interrupted for charging.

During the discharging, when the PV power output is not enough to satisfy the load, the BESS will discharge to replenish the energy difference and ensure the continuity of power supply. When there is a sudden increase in PV output, the BESS discharge may be reduced or stopped to allow as much PV energy as possible to be supplied directly to the load.

Load effects on battery charging and discharging.
During the charging, if there is a sudden drop in load, the PV or other generation source may produce excess power, and the BESS can use this extra power for charging. In the case of a sudden increase in load, the charging of the BESS may be delayed or interrupted to prioritize the load demand.

During the discharging, when there is a sudden increase in load, especially when there is insufficient PV generation or no PV generation at night, the BESS may need to be discharged to meet the additional energy demand. If the load decreases, the discharge of the BESS may be slowed or paused to extend battery life and reduce unnecessary energy loss.

Upon examination of the provided visualizations for both the generators and batteries, several observations can be made regarding their operational patterns and behaviors. The generator graphs indicate fluctuations in both active and reactive power over time, with some exhibiting more pronounced variances than others. Specifically, Generators 2 and 5 showcase noticeable active power peaks, suggesting potential high-load periods or increased demand.

Conversely, the battery charging and discharging patterns appear consistent across the board, reflecting a well-coordinated strategy. Batteries 1, 2, and 3 all demonstrate sinusoidal patterns of power flow, indicating systematic charging and discharging cycles. The amplitude differences among the batteries highlight their distinct power capacities, with Battery 3 having the highest range nearing 2.5 kW.

Integrating these observations, it can be inferred that while the generators are subjected to variable operational demands, the batteries seem to be optimized for regular charging and discharging cycles, potentially serving as a buffer or support system during peak demands or low-generation periods. The consistency in the battery patterns hints at a well-balanced energy management strategy, ensuring stability and efficiency in the overall system. Future endeavors should delve deeper into understanding the drivers behind these patterns and determining ways to further optimize energy production and storage for enhanced system reliability and performance.

```
Optimization terminated: average change in the fitness value less than options.FunctionTolerance.
  -4.8965e+08
```

Figure17. Optimal cost of BESS

The optimization process to determine the optimal cost of BESS has been completed and the final suitability or cost is approximately -$489.65 million. Depending on the specifics of the suitability function used in the optimization model, negative values could mean cost savings or profitability.

5 Conclusion and Future Work

After a careful examination of the project, we can see several power system operating modes and behaviors. The BFS and GA optimization are essential tools for energy system analysis and optimization as technology develops. To ensure the effective operation of power systems, the GA optimization algorithm, which simulates the concepts of natural selection and genetics, provides a potent tool for grid configuration, energy distribution, and demand forecasting. By use of forward and backward scanning, the BFS algorithm, which is tailored for analyzing distribution networks, guarantees grid stability and dependability.

Furthermore, the electricity system gains more stability and flexibility with the deployment of dispersed grids. Distributed networks are more resilient to uncertainties than typical centralized grids, including variations in the supply of renewable energy and unforeseen spikes in demand for power. By using the previously mentioned optimization techniques, we can better manage and control these tiny, scattered power sources, guaranteeing power supply continuity and stability. In conclusion, by combining distributed grid technology, the BFS algorithm, and the GA optimization algorithm, we can create a more dependable, efficient power system that is equipped to handle upcoming difficulties. The electricity business has a lot of promise and excellent chances in the future with ongoing technical improvements and research.

While this research offers useful insights, further work can help deepen understanding of microgrid systems and their evolving role in sustainable energy transitions. Specific areas for future investigation include:

- Exploring additional integration and control strategies to optimize the renewables mix and enhance reliability in islanded microgrids. Advanced forecasting of load demands and renewable generation could bolster these efforts.
- Investigating the impacts of wide scale microgrid deployment on the bulk power system, including assessing synergies with centralized generation and modeling aggregate grid

interactions.

- Evaluating microgrid performance through pilot studies and field demonstrations, particularly in remote communities, to quantify actual benefits and limitations.
- Performing techno-economic analyses for microgrid projects to determine sustainability, identify cost bottlenecks, and guide commercialization.
- Assessing microgrid cybersecurity risks as integration and automation increase. Strategies are needed to guard against vulnerabilities.
- Developing advanced computational tools to assist in microgrid design, optimization and real-time control. Machine learning and artificial intelligence techniques may hold promise.
- Examining the policy, regulatory and business model adaptations required to support accelerated microgrid growth. Key considerations include tariffs, interconnection rules, and market participation.

Reference

[1] Branco, H., Castro, R., & Lopes, A. S. (2018). Battery energy storage systems as a way to integrate renewable energy in small, isolated power systems. Energy for Sustainable Development, 43, 90-99.

[2] Domínguez-Barbero, D., García-González, J., Sanz-Bobi, M. A., & Sánchez-Úbeda, E. F. (2020). Optimising a microgrid system by deep reinforcement learning techniques. Energies, 13(11), 2830.

[3] Duan, J., Yi, Z., Shi, D., Lin, C., Lu, X., & Wang, Z. (2019). Reinforcement-learning-based optimal control of hybrid energy storage systems in hybrid AC–DC microgrids. IEEE Transactions on Industrial Informatics, 15(9), 5355-5364.

[4]Du, Y., & Li, F. (2019). Intelligent multi-microgrid energy management based on deep neural network and model-free reinforcement learning. IEEE Transactions on Smart Grid, 11(2), 1066-1076.

[5] Ghasemi, A., Mortazavi, S. S., & Mashhour, E. (2016). Hourly demand response and battery energy storage for imbalance reduction of smart distribution company embedded with electric vehicles and wind farms. Renewable Energy, 85, 124-136.

[6] Gomes, J. G., Xu, H. J., Yang, Q., & Zhao, C. Y. (2021). An optimization study on a typical renewable microgrid energy system with energy storage. Energy, 234, 121210.

[7] Geleta, D. K., & Manshahia, M. S. (2021). Artificial bee colony-based optimization of hybrid wind and solar renewable energy system. In Research Anthology on Clean Energy Management and Solutions (pp. 819-842). IGI Global.

[8] Ishraque, M. F., Shezan, S. A., Ali, M. M., & Rashid, M. M. (2021). Optimization of load dispatch strategies for an islanded microgrid connected with renewable energy sources. Applied Energy, 292, 116879.

[9] Jayanetti, A., Halgamuge, S., & Buyya, R. (2022). Deep reinforcement learning for energy and time optimized scheduling of precedence-constrained tasks in edge–cloud computing environments. Future Generation Computer Systems, 137, 14-30.

[10] Ji, Y., Wang, J., Xu, J., & Li, D. (2021). Data-driven online energy scheduling of a microgrid based on deep reinforcement learning. Energies, 14(8), 2120.

[11] Khan, A. A., Naeem, M., Iqbal, M., Qaisar, S., & Anpalagan, A. (2016). A compendium of optimization objectives, constraints, tools and algorithms for energy management in microgrids. Renewable and Sustainable Energy Reviews, 58, 1664-1683.

[12] Keane, A., Ochoa, L. F., Borges, C. L., Ault, G. W., Alarcon-Rodriguez, A. D., Currie, R. A., ... & Harrison, G. P. (2012). State-of-the-art techniques and challenges ahead for distributed generation planning and optimization. IEEE Transactions on Power Systems, 28(2), 1493-1502.

[13] Li, P., Xu, D., Zhou, Z., Lee, W. J., & Zhao, B. (2015). Stochastic optimal operation of microgrid based on chaotic binary particle swarm optimization. IEEE Transactions on Smart Grid, 7(1), 66-73.

[14] Nair, U. R., & Costa-Castelló, R. (2020). A model predictive control-based energy management scheme for hybrid storage system in islanded microgrids. IEEE access, 8, 97809-97822.

[15] Parisio, A., Rikos, E., & Glielmo, L. (2014). A model predictive control approach to microgrid operation optimization. IEEE Transactions on Control Systems Technology, 22(5), 1813-1827.

[16] Raghavan, A., Maan, P., & Shenoy, A. K. (2020). Optimization of day-ahead energy storage system scheduling in microgrid using genetic algorithm and particle swarm optimization. Ieee Access, 8, 173068-173078.

[17] Ryan, D. J., Razzaghi, R., Torresan, H. D., Karimi, A., & Bahrani, B. (2020). Grid-supporting battery energy storage systems in islanded microgrids: A data-driven control approach. IEEE Transactions on Sustainable Energy, 12(2), 834-846.

[18] Sharma, I., Dong, J., Malikopoulos, A. A., Street, M., Ostrowski, J., Kuruganti, T., & Jackson, R. (2016). A modeling framework for optimal energy management of a residential building. Energy and Buildings, 130, 55-63.

[19] UNDRE, V. S. (2019). Highly renewable energy integrated grid analysis and islanded microgrid balancing by battery energy storage system.

[20] Xu, X., Jia, Y., Xu, Y., Xu, Z., Chai, S., & Lai, C. S. (2020). A multi-agent reinforcement learning-based data-driven method for home energy management. IEEE Transactions on Smart Grid, 11(4), 3201-3211.

[21] Ye, Y., Qiu, D., Wu, X., Strbac, G., & Ward, J. (2020). Model-free real-time autonomous control for a residential multi-energy system using deep reinforcement learning. IEEE Transactions on Smart Grid, 11(4), 3068-3082.